Original Article

JCBFM

Journal of Cerebral Blood Flow & Metabolism
2017, Vol. 37(10) 3401–3408

DOI: 10.1177/0271678X17696322
journals.sagepub.com/home/jcbfm
SAGE

Imaging angiogenesis using ^{68}Ga-NOTA-PRGD2 positron emission tomography/computed tomography in patients with severe intracranial atherosclerotic disease

Shi Shu[1,*], Li Zhang[1,*], Yi Cheng Zhu[1], Fang Li[2], Li Ying Cui[1], Hao Wang[2], Yi Sun[2], Pei Lin Wu[2,3], Zhao Hui Zhu[2,*] and Bin Peng[1,*]

Abstract

Angiogenesis is a critical compensation route, which has been demonstrated in the brain following ischemic stroke; however, few studies have investigated angiogenesis in chronic intracranial atherosclerosis disease (ICAD). We used ^{68}Ga-NOTA-PRGD2 positron emission tomography/computed tomography based imaging to detect angiogenesis in chronic ICAD and to explore the factors that may have affected it. A total of 21 participants with unilateral severe chronic ICAD were included in the study. Of the 21 participants, 19 were men; the mean (SD) age was 52 (15) years. In 18 participants, we observed elevated ^{68}Ga-NOTA-PRGD2 uptake in the peri-infarct, subcortical, and periventricular regions of the lesioned side, with a higher ^{68}Ga-NOTA-PRGD2 SUV_{max} compared to that in the contralateral hemisphere (0.15 vs. 0.06, p=0.001). The ^{18}F-FDG PET SUV_{max} was significantly lower on the lesioned side (11.28 vs. 13.92, p=0.001). Subgroup analyses revealed that the recent group (<6 months) had a higher lesion-to-contralateral region ratio SUV_{max} than the remote group (>6 months) (6.73 vs. 2.36, p<0.05). Our results provide molecular imaging evidence of angiogenesis in patients with severe chronic ICAD. Furthermore, the extent of angiogenesis in chronic ICAD may be affected by the post-qualified event time interval, and not by infarction itself or the severity of the arterial lesion.

Keywords

Angiogenesis, ^{68}Ga-NOTA-PRGD2 PET/CT, chronic ischemia, severe intracranial atherosclerosis disease, collaterals

Received 14 October 2016; Revised 12 January 2017; Accepted 24 January 2017

Introduction

Intracranial atherosclerotic disease (ICAD) is one of the most common causes of ischemic stroke worldwide.[1,2] The risk of recurrent ipsilateral stroke is higher in patients with high-grade stenosis (≥70%) than in those with less severe stenosis (<70%).[3] Hemodynamic impairment and thromboembolism caused by ICAD may lead to the recruitment of collaterals, which can improve the perfusion state of the ischemic brain.[4–6] Collateral circulation, thus, becomes an important factor not only in predicting prognosis in cases of acute ischemic stroke, but also identifying

[1]Department of Neurology, Peking Union Medical College Hospital, Chinese Academy of Medical Science and Peking Union Medical College, Beijing, China
[2]Department of Nuclear Medicine, Peking Union Medical College Hospital, Chinese Academy of Medical Science and Peking Union Medical College, Beijing, China
[3]Department of Nuclear Medicine, Dong Zhi Men Hospital, Beijing University of Chinese Medicine, Beijing, China

*These authors contributed equally to the article.

Corresponding author:
Bin Peng, Department of Neurology, Peking Union Medical College Hospital, Chinese Academy of Medical Science and Peking Union Medical College, Beijing, China.
Email: pengbin3@hotmail.com

patients at high risk of stroke following chronic severe ICAD.[7,8]

Two classes of collaterals are activated by hypoperfusion or ischemia in the brain, the primary collaterals consisting of arteries included in the circle of Willis circle, and the secondary collaterals, including the leptomeningeal and ophthalmic anastomoses developing from preexisting arterioles as well as through angiogenesis, i.e. the formation of new blood vessels.[9] Current studies of collateral supply in ICAD focus primarily on the circle of Willis and the anastomoses, which maintain the blood supply.[10–12] Although angiogenesis in acute ischemic stroke is known to be a critical intrinsic restoration mechanism and regarded as a potential treatment strategy, angiogenesis in chronic ICAD is less studied.[13,14]

Animal studies of chronic cerebral hypoxia or hypoperfusion have identified angiogenesis by detecting increases in the serum vascular endothelial growth factor (VEGF) levels and the microvessel density.[15–17] In addition, investigators have found that patients with severe ICAD show increased level of serum endothelial progenitor cells,[14,18] which play an important role in angiogenesis. However, conclusions from animal research are limited by the difficulty to simulate complex pathophysiological processes; results from serum-based clinical studies are questioned given the restrictions imposed by the blood–brain barrier (BBB).[14]

With the rapid development of molecular imaging techniques, angiogenesis imaging in tumors and ischemic diseases is experiencing a breakthrough.[19,20] ^{68}Ga-NOTA-PRGD2 (NOTA-PRGD2 is NOTA-PEG4-E[c(RGDfK)]$_2$), a ^{68}Ga radiolabeled cyclic arginine-glycine-aspartic acid (RGD) dimer with PEG spacers, can specifically and efficiently combine with integrin $\alpha v\beta 3$.[21–24] Integrin $\alpha v\beta 3$ is specifically expressed on the surface of activated endothelial cells, and not quiescent ones, during the process of angiogenesis;[25–27] therefore, the aggregation of ^{68}Ga-NOTA-PRGD2 in the brain detected by positron emission tomography (PET) can be used as an indicator of angiogenesis in the examined tissue. ^{68}Ga-NOTA-RGD has been translated into clinical application to examine angiogenesis in moyamoya disease, acute myocardial infarction, and acute ischemic stroke via PET/computed tomography (CT).[28,29] This approach was superior in the context of radionuclide production and image accuracy compared to other angiogenesis imaging methods.

The primary aim of this study is to provide molecular imaging evidence of angiogenesis in chronic ICAD using ^{68}Ga-NOTA-PRGD2 PET/CT. We compared ^{68}Ga-NOTA-PRGD2-binding in the regions supplied by the stenotic/occlusive arteries with that in the contralateral regions. We analyzed differences in ^{68}Ga-NOTA-PRGD2 uptake between different subgroups to evaluate factors such as the severity of the artery lesion, qualifying infarcts, and intervals between qualifying events and PET scans, which may have an effect on angiogenesis.

Methods

Subjects

This pilot study conformed to ethical standards of Helsinki Declaration and was approved by the Institutional Review Boards of the Peking Union Medical College Hospital, Chinese Academy of Medical Sciences, and Peking Union Medical College. Each participant provided written informed consent prior to participation in the study. All the patients underwent ^{68}Ga-NOTA-PRGD2 PET/CT and ^{18}F- fluorodeoxyglucose (FDG) PET/CT scans within one week. The inclusion criteria were as follows: (1) age between 18 and 80 years, and (2) unilateral intracranial internal carotid, middle cerebral artery, or anterior cerebral artery stenosis of over 70% detected by magnetic resonance or computed tomography angiography (MRA or CTA), or of over 50% detected by digital subtraction angiography (DSA). The exclusion criteria were as follows: emboligenic cardiopathy, transient ischemic attack (TIA), or stroke within 30 days; neoplasm; inflammatory conditions; nonatherosclerotic causes of intracranial stenosis; pregnancy; lactation period; and impaired renal or liver function. None of the patients received stenting treatment. Patients who underwent PET/CT scans within 6 months (more than 1 month at the same time) of experiencing ischemic events, including transient ischemic attack and stroke, were assigned to the recent group; while those who underwent PET/CT scans 6 months after the ischemic events were assigned to remote group.

PET/CT scanning

^{68}Ga-NOTA-PRGD2 was prepared as previously reported.[21,28] ^{68}Ga-NOTA-PRGD2 was injected intravenously at a dose of 1.85 MBq (0.05 mCi) per kilogram of body weight ($\leq$20 μg/NOTA-PRGD2). Thirty minutes later,[30–32] a low-dose CT scan (140 kV, 35 mA, pitch 1:1, layer 3 mm, layer spacing 3 mm, matrix 512×512, FOV 70 cm) was first performed for attenuation correction and anatomical localization. This was followed by PET scans (one 10-min bed position, FWHM 3 mm, matrix 336×336, zoom 2) using an iterative algorithm (six iterations for the brain). The reconstructed voxel dimension is 1 mm.

All patients underwent ^{18}F-fluorodeoxyglucose (FDG) imaging within 1 week of the ^{68}Ga-NOTA-PRGD2 PET imaging. Patients were required to fast

for at least 6 h before the ^{18}F-FDG PET/CT scan to decrease the background radionuclide uptake by the brain. For each patient, 5.55 MBq (0.15 mCi) of ^{18}F-FDG per kilogram of body weight was injected intravenously. The PET/CT scans were acquired approximately 2 h after the ^{18}F-FDG injection, with a 10-minute bed position maintained for the PET scans. All the PET/CT scans in this study were acquired on the Biograph 64 Truepoint TrueV PET/CT system (Siemens Medical Solutions, Erlangen, Germany).

Image analysis

The ^{68}Ga-NOTA-PRGD2 and ^{18}F-FDG PET/CT images were transferred to a workstation (MMWP, Siemens Medical Solution) for performing comparison and analysis. Three blinded independent nuclear medicine experts assessed the PET/CT images and reached a consensus in case of discordance. A semi-quantitative analysis was conducted by the same physicians. Only the maximum standardized uptake value (SUV_{max}) was recorded for the ^{68}Ga-NOTA-PRGD2 PET images. The regions of interest (ROIs) were kept away from regions near the meningeal vessels and the choroid plexus in ventricle in three dimensions. The SUV_{max} of a symmetrical ROI in the contralateral region was measured, and the lesion-to-contralateral region ratio (LCR) was calculated. For the ^{18}F-FDG PET images, the ROIs were drawn over the cortical territories or subcortical nuclei irrigated by the stenotic arteries, and the SUV_{max} values were recorded. The contralateral ROIs were drawn symmetrically.

Statistical analysis

The Kolmogorov–Smirnov test was used to test the normality of the distribution. The differences in the ^{68}Ga-NOTA-PRGD2 SUV_{max} or ^{18}F-FDG SUV_{max} were compared between the lesion and contralateral sides using the Wilcoxon rank sum test. The LCRs were compared between the recent and remote groups using the Mann–Whitney test. The same method was used to compare the LCRs between the stenotic and occlusive groups, as well as to qualify the infarction-positive and negative groups. All the statistical analyses were performed using Statistical Package for Social Sciences (SPSS), version 22.0, SPSS Inc., Chicago, USA. Results with $p<0.05$ were considered to be statistically significant.

Results

^{68}Ga-NOTA-PRGD2 distribution and uptake patterns

The demographic information of the cohort is provided in Table 1. The ^{68}Ga-NOTA-PRGD2 uptake was evaluated 30 min after the intravenous injection, when the blood pool background was relatively low. According to the independent analysis from the three nuclear medicine physicians, ^{68}Ga-NOTA-PRGD2 uptake was identified in 18 out of the 21 patients. Except for the choroid plexus, the normal brain had no uptake of ^{68}Ga-NOTA-PRGD2 (Figure 1(i) to (l). Abnormal ^{68}Ga-NOTA-PRGD2 uptake aggregated in a patchy format around the site of infarction (Figure 1(a) to (d)), or in a puncta format in the periventricular zones and subcortical nuclei without a lesion, which must be irrigated by the stenotic arteries (Figure 1(e) to (h)).

Table 1. Demographic characteristics.

Characteristic	Value
No.	21
Age, mean (SD); *y*	52.6 (±15.2)
Male; *n*	19
Other medical illness; *n*	
Hypertension	11
Diabetes mellitus	5
Dyslipidemia	8
Smoking habit; *n*	8
Qualifying event; *n* (stroke/TIA)	14 (10/4)
Qualifying artery (occlusion/stenosis)	15/6
Intracranial ICA; *n* (occlusion/stenosis)	4 (3/1)
MCA; *n* (occlusion/stenosis)	16 (11/5)
ACA occlusion; *n*	1
Post-qualified event time interval; *n* (recent/remote)	14 (4/10)

SD: standard deviation; ICA: intracranial carotid artery; MCA: middle cerebral artery; ACA: anterior cerebral artery.

In patients with ICAD (N=21), the ^{68}Ga-NOTA-PRGD2 SUV_{max} was elevated on the lesion side compared to that on the contralateral side, while the ^{18}F-FDG SUV_{max} was significantly lower in the lesion side than in the contralateral side (Table 2).

Effects of the infarction lesion on radiotracer uptake

The subgroup analyses were performed by dividing the cohort into subgroups according to different parameters. The patients were divided into two groups according to the presence of the infarction lesion. In patients with an infarction lesion, the ^{18}F-FDG SUV_{max} was lower on the stenotic/occlusive artery side compared to that on the contralateral side; in contrast, the ^{68}Ga-NOTA-PRGD2 SUV_{max} was higher. In patients without the infarction lesion, the

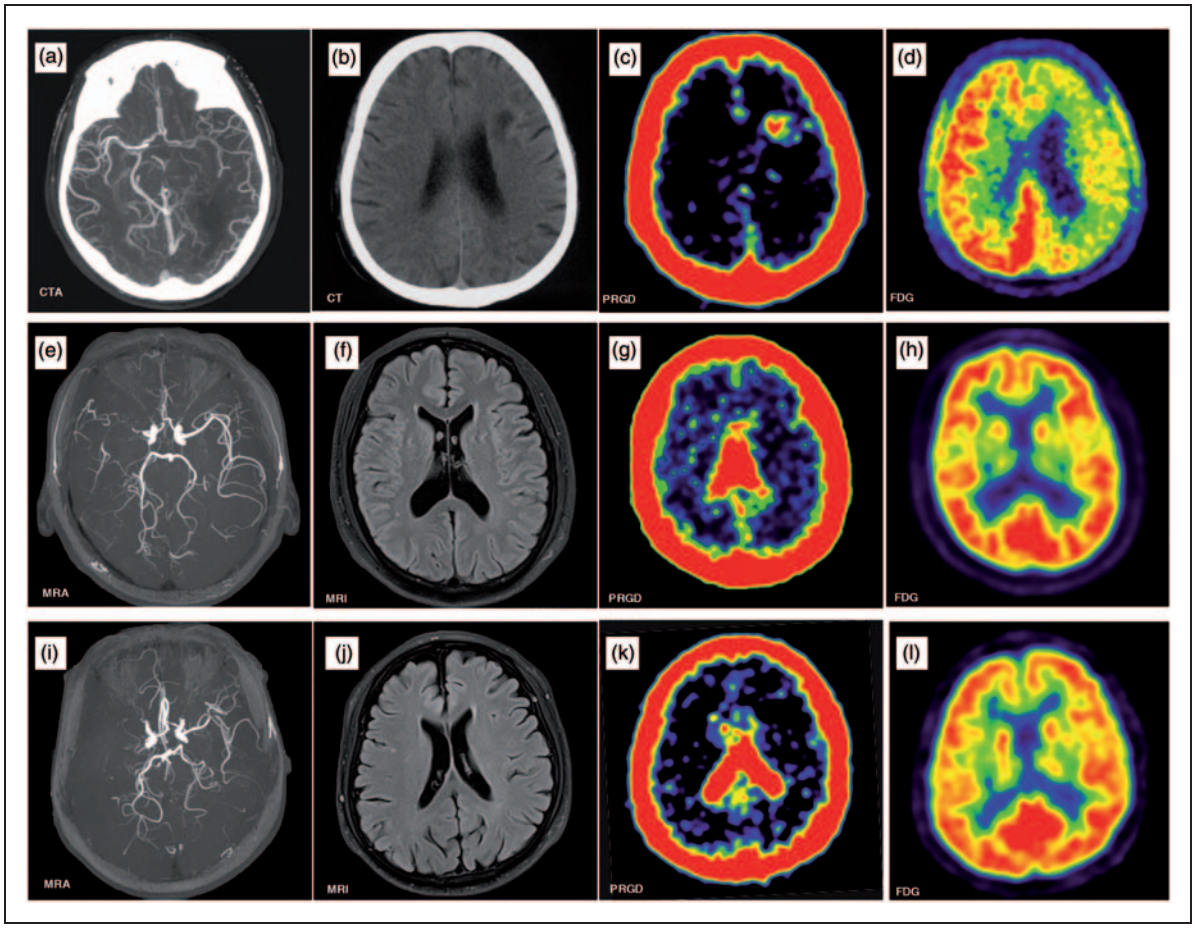

Figure 1. Upper row: CTA in a 64-year-old man revealed severe stenosis of the left middle cerebral artery (MCA) (a), brain CT showed left frontal lobe infarction (b). PET/CT scan showed accumulation of ^{68}Ga-NOTA-PRGD2 around the infarct area (c) with a diffuse decrease in the metabolism (yellow arrow) in ^{18}F-fluorodeoxyglucose (FDG) PET (d) 33 days after ischemic stroke. Middle row: A 44-year-old man had an ischemic stroke 72 months prior to enrolment, leaving numbness in his left arm. MRA revealed right MCA occlusion (e). No significant infarcts were seen on the MRI (f). The ^{68}Ga-NOTA-PRGD2 uptake was found in a puncta-like form scattered over the subcortical areas (g, yellow arrow), although no significant difference for ^{18}F-FDG PET was seen between the lesioned and contralateral sides (h). Lower row: A 70-year-old man had an ischemic stroke 22 years prior to enrolment, leaving weakness in the right leg. MRA showed left MCA occlusion (i). No infarct was observed on the MRI (J). The ^{68}Ga-NOTA-PRGD2 PET and ^{18}F-FDG PET uptakes were not significantly different between the lesioned and contralateral sides (k, l).
CTA: computed tomography angiography; PET: positron emission tomography; CT: computed tomography; MRI: magnetic resonance imaging; MRA: magnetic resonance angiography.

^{68}Ga-NOTA-PRGD2 SUV_{max} on the stenotic/occlusive side was higher than that on the contralateral side, while the SUV_{max} values for ^{18}F-FDG were similar. The LCR of the ^{18}F-FDG SUV_{max} in patients with an infarction lesion was lower than in patients without a lesion; the LCR of the ^{68}Ga-NOTA-PRGD2 SUV_{max} was not significantly different between the two groups (Table 2).

Effects of the severity of the lesion on radiotracer uptake

According to the severity of the affected arteries, we divided the patients into the occlusive and stenotic groups (≥70% stenosis). There was no significant difference between the ^{18}F-FDG SUV_{max} values for the lesion and contralateral sides in each group; however, both the groups had a higher ^{68}Ga-NOTA-PRGD2 SUV_{max} value on the lesion side than that on the contralateral side. Moreover, the LCRs of both the ^{68}Ga-NOTA-PRGD2 SUV_{max} and ^{18}F-FDG SUV_{max} were similar between the occlusion and stenosis groups (Table 2).

Effects of the post-qualified event interval on radiotracer uptake

A total of 14 subjects had qualifying events; four of these patients were in the recent group and 10 patients

Table 2. Subgroup analysis of ^{68}Ga-NOTA-PRGD2 and ^{18}F-FDG PET imaging.

		RGD_{max}				FDG_{max}			
Group	Total	Lesion	Contralateral	*p*	LCR	Lesion	Contralateral	*p*	LCR
Overall	*N*=21	0.15 (0.05–0.64)	0.06 (0.03–0.11)	0.001	2.6 (0.75–10.67)	11.28 (2.73–21.11)	13.92 (6.44–26.77)	0.001	0.92 (0.21–10.05)
Qualifying infarction*									
Yes	*N*=7	0.17 (0.11–0.64)	0.06 (0.03–0.07)	0.017	3.00 (2.00–10.67)	5.52 (2.73–11.09)	13.92 (7.37–26.77)	0.018	0.53 (0.21–0.85)
No	*N*=14	0.155 (0.06–0.29)	0.06 (0.03–0.11)	<0.003	2.81 (1.50–4.00)	12.76 (5.79–21.11)	13.5 (6.44–21)	0.069	0.96 (0.87–1.05)
Severity of the qualifying artery									
O	*N*=15	0.16 (0.06–0.64)	0.06 (0.03–0.11)	0.001	3.00 (0.75–10.67)	11.09 (2.73–21.11)	14.37 (6.5–26.77)	0.005	0.92 (0.21–1.04)
S	*N*=6	0.13 (0.06–0.21)	0.06 (0.05–0.10)	0.042	1.90 (1.00–2.63)	12.17 (4.96–16.23)	13.28 (6.44–18.69)	0.116	0.93 (0.36–1.05)
Months from qualifying event to PET scans**									
<6 m	*N*=4	0.24 (0.13–0.64)	0.05 (0.03–0.06)	0.125	6.73 (2.60–10.67)	6.53 (2.73–13.30)	14.15 (7.37–15.42)	0.125	0.47 (0.36–0.86)
>6 m	*N*=10	0.14 (0.09–0.21)	0.06 (0.03–0.11)	0.007	2.36 (0.90–3.67)	11.19 (4.3–17.23)	12.47 (6.5–26.77)	0.017	0.89 (0.21–1.05)

LCR: lesion to contralateral ratio; O: occlusion; S: stenosis; FDG_{max}: maximum value of ^{18}F-fluorodeoxyglucose; RGD_{max}: radiolabeled cyclic arginine-glycine-aspartic acid. The values in parentheses indicate the range for the data. *$p<0.001$, FDG_{max} LCR comparison between subjects with a qualifying infarction and those without infarction; **$p=0.014$ and $p=0.052$, RGD_{max} LCR and FDG_{max} LCR between the recent (<6 m) vs. remote (>6 m) groups, respectively.

were in the remote group. For the recent group, the ^{68}Ga-NOTA-PRGD2 SUV_{max} on the lesion side is higher than that on the contralateral side; the ^{18}F-FDG SUV_{max} was lower on the lesion side, but neither of them reached statistical significance. For the remote group, the ^{68}Ga-NOTA-PRGD2 SUV_{max} and ^{18}F-FDG SUV_{max} between the lesioned and contralateral sides were significantly different. The LCR of the ^{68}Ga-NOTA-PRGD2 SUV_{max} in the recent group was higher compared to that of the remote group, and an opposite effect was observed for the LCR of the ^{18}F-FDG SUV_{max}. However, only the former reached apparent significance (Table 2).

Discussion

The present study demonstrated an increased uptake of ^{68}Ga-NOTA-PRGD2 on the lesion side compared to that on the contralateral side, which indicates that angiogenesis occurs in the territory irrigated by the stenotic/occlusive artery. Integrin αvβ3 imaging has been proved to be a valuable tool for angiogenesis assessment in various diseases by previous studies.[13,28,29,33] The ^{68}Ga-labeled RGD dimer, ^{68}Ga-NOTA-PRGD2, has gained popularity for clinical application given its ease of preparation, in addition to its high specificity and affinity for integrin αvβ3.[23,34] Jeong et al.[29] showed that ^{68}Ga-RGD could be blocked by cold RGD both in an *in vitro* binding assay and in an animal model, which demonstrated its specific binding to integrin αvβ3. Several clinical studies[28,33] as well as our previous study[35] found moderate uptake of ^{68}Ga-NOTA-PRGD2 in the choroid plexus, but no uptake in the normal cerebral parenchyma. Therefore, the abnormal ^{68}Ga-NOTA-PRGD2 uptake we observed in the cerebral parenchyma strongly suggested angiogenesis in patients with ICAD.

Angiogenesis as a crucial restorative mechanism under ischemic conditions and has been widely studied in acute ischemic diseases; however, few studies have investigated angiogenesis in chronic ischemia. Prior chronic cerebral hypoxia studies in animals and serum-based studies in patients with ICAD and moyamoya disease have indicated the occurrence of angiogenesis in chronic cerebral ischemia.[15–17] In this study, we directly imaged angiogenesis using ^{68}Ga-NOTA-PRGD2 PET/CT beyond the acute phase in patients with severe ICAD. To the best of our knowledge, ours is the first study to evaluate the collateral circulation route at the level of angiogenesis *in vivo*. This approach may provide a new way for further assessment of collateral circulation in chronic intracranial artery disease.

Choi et al.[29] were first to use ^{68}Ga-RGD PET/CT to observe angiogenesis following acute cerebral infarct in pediatric patients with moyamoya disease. Next, Sun et al.[28] applied ^{68}Ga-RGD PET/CT to investigate angiogenesis in a different group of patients with acute embolic stroke. In this study, all the PET scans were performed more than 1 month after the qualifying events to avoid the influence of acute stroke on angiogenesis. Compared to the acute phase after stroke in previous studies, the uptake of ^{68}Ga-NOTA-PRGD2 in chronic ICAD from our study is weaker. Moreover, the ^{68}Ga-NOTA-PRGD2 uptake is not only limited to areas around the infarct zone, but also scatters over the region supplied by the affected artery in a puncta-like form. It is different from previous observations in patients with acute infarcts, according to which, the ^{68}Ga-NOTA-PRGD2 uptake is significantly elevated surrounding the infarct and shows a patchy form. Furthermore, compared to patients without an infarction lesion, patients with lesions exhibited decreased LCR FDG_{max} values but similar LCR RGD_{max} values, which confirms that the ^{68}Ga-NOTA-PRGD2 uptake in our cohort is not related to the presence of the lesion.

Many factors may affect angiogenesis process. In this study, we also compared patients with different post-qualified event time intervals, and found that the LCR RGD_{max} of the recent group was significantly higher than that of the remote group. This is consistent with the conclusion that angiogenesis decreases as the post-qualified event time increases in studies of angiogenesis in acute ischemic stroke.[28,36] In addition, we also investigated whether the severity of the artery lesion affects the ^{68}Ga-NOTA-PRGD2 uptake, and found that the LCR RGD_{max} values are similar between the occlusive and stenotic groups, which demonstrates that the angiogenesis detected by ^{68}Ga-NOTA-PRGD2 is not associated with the severity of the artery lesion. A previous study has also shown that several patients with occlusive arteries never experience any ischemic event, and that chronic hemodynamic compromise, rather than the severity of the lesion in the arteries, may be a predictor of ischemic events in those patients.[37] Combined with the results of that study, our results showing no difference in the ^{68}Ga-NOTA-PRGD2 uptake between the occlusive and stenotic groups, also suggest that angiogenesis indicating hemodynamic impairment, rather than severity of the arterial lesion, has the potential to be a sensitive predictor of clinical outcomes of patients with ICAD. Finally, cerebrovascular risk factors, such as hypertension, diabetes, and hypercholesterolemia, are reported to have deleterious effects on post-ischemic angiogenesis.[38] A larger sample size and more accurate grouping in future studies are needed to evaluate the impact of these confounding factors.

According to the findings of the study, we hypothesized that angiogenesis might be a biomarker reflecting the extent of compensation of collateral circulation in chronic ICAD. Prior studies have shown that angiogenesis can be induced by hypoperfusion in chronic cerebral ischemia.[16,39] The status of cerebral perfusion might affect the process of angiogenesis in chronic ICAD. Further work is needed to identify the exact mechanism of angiogenesis in ICAD.

The evaluation of angiogenesis in patients with ICAD might provide more information about the prognosis and adaptation of treatment targeting angiogenesis. There has been a debate about the role of angiogenesis during stroke recovery for a long time.[40,41] In patients with ICAD, angiogenesis in addition to collateral circulation could be beneficial for an improved clinical outcome by restoring the blood supply of areas irrigated by the lesioned arteries. It is equally true that angiogenesis may indicate insufficiency compensation of the collaterals, representing a bad prognosis, as it is deemed to be induced by hypoperfusion or ischemia. Therefore, further evaluation of the correlation between ^{68}Ga-NOTA-PRGD2 and clinical outcome would be useful. In addition, therapies promoting angiogenesis have been seen to improve the outcomes of experimental stroke in mice, but the current results from clinical trials are not encouraging.[38] With the application of molecular imaging of angiogenesis using ^{68}Ga-NOTA-PRGD2 PET/CT, further trials with different therapeutic agents and routes of administration in ICAD would become more realizable.

This pilot study has some limitations as well. First, patient selection bias might exist due to the limited sample size and imbalanced men:women ratio. However, the manner in which we collected the data from the lesion side and the contralateral side from the same patient might minimize the impact of this bias. Considering there was no previous study using ^{68}Ga-NOTA-PRGD2 PET/CT to explore angiogenesis in chronic ischemia, as well as the high of PET/CT-based applications, we need to obtain preliminary findings before planning a larger, prospective study. Second, we do not apply another radioactive tracer without integrin $\alpha v\beta 3$-binding activity to exclude the influence of the blood brain barrier, considering safety issues as well as the fact that damage to the blood brain barrier is almost restored in patients with chronic ischemia. Third, the absence of a kinetic study is also an important limitation of this study. Several previous studies analyzed the biodistribution of the ^{68}Ga-NOTA-RGD and showed that the nuclide uptake decreased rapidly during the first 30 min after injection and reached a plateau thereafter.[30–32,35,42] According to these studies, we performed the PET scans 30 min after injection; however, kinetic studies are needed in patient populations to explore the

effects of specific binding and altered cerebral blood flow on timing of semiquantitative measures. Fourth, SUV_{max} analyzed in this study is inclined to be affected by noise signal, but considering the extremely low background uptake of ^{68}Ga-NOTA-PRGD2, it is also not appropriate to choose SUV_{mean}. Finally, it should be noted that this study concentrated on the collateral compensation in chronic ICAD. There might be other processes underlying ^{68}Ga-NOTA-PRGD2 uptake, such as inflammation, but we found no evidence for inflammation on the ^{18}F-FDG PET scans, which should show increased FDG uptake in the presence of inflammation. Further studies should also investigate pro- and anti-inflammatory cytokines in patients with ^{68}Ga-NOTA-PRGD2 uptake. Despite its preliminary nature, this study can clearly and directly depict angiogenesis in the cerebral parenchyma of patients with chronic ICAD, and analyze potential factors that may have an influence on angiogenesis.

Conclusion

In conclusion, our study demonstrated angiogenesis in the chronic phase in patients with ICAD using ^{68}Ga-NOTA-PRGD2 PET/CT imaging. To date, ours is the first study to evaluate the collateral circulation route in ICAD at the level of angiogenesis *in vivo*. ^{68}Ga-NOTA-PRGD2 PET/CT imaging could be considered as a supplement in the evaluation of collateral compensation, in addition to the conventional methods used in ICAD. Further prospective studies are required in order to investigate angiogenesis among the different ICAD subgroups, as well as the relationship between angiogenesis and prognosis of patients with ICAD.

Funding

The author(s) disclosed receipt of the following financial support for the research, authorship, and/or publication of this article: This work was supported by the National Natural Science Foundation of China projects [81471246], as well as the Beijing Natural Science Foundation [7152121].

Declaration of conflicting interests

The author(s) declared no potential conflicts of interest with respect to the research, authorship, and/or publication of this article.

Authors' contributions

Shi Shu was involved in the concept and design of the study, analysis, and interpretation of the data, and drafting and revising the manuscript. Li Zhang was involved in the analysis and interpretation of the data, as well as revising the manuscript. Yi Cheng Zhu was involved in the recruitment of the subjects. Fang Li supervised the study. Li Ying Cui was involved in study supervision and subject recruitment. Hao Wang, Yi Sun, and Pei Lin Wu were involved in the acquisition and analysis of the data, and administrative, technical, or material support. Zhao Hui Zhu was involved in study supervision, concept, and design of the study, technical support, interpretation of the data, and revising the manuscript. Bin Peng was involved in study supervision and obtaining funding, as well as in the concept and design of the study. Shi Shu, Li Zhang, Zhao Hui Zhu, and Bin Peng have contributed equally to this article.

References

1. Wong KS. Global burden of intracranial atherosclerosis. *Int J Stroke* 2006; 1: 158–159.
2. Gorelick PB, Wong KS, Bae HJ, et al. Large artery intracranial occlusive disease: A large worldwide burden but a relatively neglected frontier. *Stroke* 2008; 39: 2396–2399.
3. Kasner SE, Chimowitz MI, Lynn MJ, et al. Predictors of ischemic stroke in the territory of a symptomatic intracranial arterial stenosis. *Circulation* 2006; 113: 555–563.
4. Kim JS, Nah HW, Park SM, et al. Risk factors and stroke mechanisms in atherosclerotic stroke: Intracranial compared with extracranial and anterior compared with posterior circulation disease. *Stroke* 2012; 43: 3313–3318.
5. Chen H, Hong H, Liu D, et al. Lesion patterns and mechanism of cerebral infarction caused by severe atherosclerotic intracranial internal carotid artery stenosis. *J Neurol Sci* 2011; 307: 79–85.
6. Martinon E, Lefevre PH, Thouant P, et al. Collateral circulation in acute stroke: Assessing methods and impact: A literature review. *J Neuroradiol* 2014; 41: 97–107.
7. Nishijima Y, Akamatsu Y, Weinstein PR, et al. Collaterals: Implications in cerebral ischemic diseases and therapeutic interventions. *Brain Res* 2015; 1623: 18–29.
8. Bang OY, Goyal M and Liebeskind DS. Collateral circulation in ischemic stroke: Assessment tools and therapeutic strategies. *Stroke* 2015; 46: 3302–3309.
9. Liebeskind DS. Collateral circulation. *Stroke* 2003; 34: 2279–2284.
10. Liebeskind DS, Cotsonis GA, Saver JL, et al. Collaterals dramatically alter stroke risk in intracranial atherosclerosis. *Ann Neurol* 2011; 69: 963–974.
11. Liebeskind DS, Cotsonis GA, Saver JL, et al. Collateral circulation in symptomatic intracranial atherosclerosis. *J Cereb Blood Flow Metab* 2011; 31: 1293–1301.
12. Choi JW, Kim JK, Choi BS, et al. Angiographic pattern of symptomatic severe M1 stenosis: Comparison with presenting symptoms, infarct patterns, perfusion status, and outcome after recanalization. *Cerebrovasc Dis* 2010; 29: 297–303.
13. Menezes LJ, Kotze CW, Agu O, et al. Investigating vulnerable atheroma using combined (18)F-FDG PET/CT angiography of carotid plaque with immunohistochemical validation. *J Nucl Med* 2011; 52: 1698–1703.
14. Massot A, Navarro-Sobrino M, Penalba A, et al. Decreased levels of angiogenic growth factors in intracranial atherosclerotic disease despite severity-related

increase in endothelial progenitor cell counts. *Cerebrovasc Dis* 2013; 35: 81–88.
15. Hai J, Li S-T, Lin Q, et al. Vascular endothelial growth factor expression and angiogenesis induced by chronic cerebral hypoperfusion in rat brain. *Neurosurgery* 2003; 53: 963–972.
16. Jing Z, Shi C, Zhu L, et al. Chronic cerebral hypoperfusion induces vascular plasticity and hemodynamics but also neuronal degeneration and cognitive impairment. *J Cereb Blood Flow Metab* 2015; 35: 1249–1259.
17. Oldendorf WH. Trhophic changes in the arteries at the base of the rat brain in response to bilateral common carotid ligation. *J Neuropathol Exp Neurol* 1989; 48: 534–547.
18. Sobrino T, Perez-Mato M, Brea D, et al. Temporal profile of molecular signatures associated with circulating endothelial progenitor cells in human ischemic stroke. *J Neurosci Res* 2012; 90: 1788–1793.
19. Backer MV and Backer JM. Imaging key biomarkers of tumor angiogenesis. *Theranostics* 2012; 2: 502–515.
20. Cai W, Guzman R, Hsu AR, et al. Positron emission tomography imaging of poststroke angiogenesis. *Stroke* 2009; 40: 270–277.
21. Li Z-B, Chen K and Chen X. ^{68}Ga-labeled multimeric RGD peptides for microPET imaging of integrin αvβ3 expression. *Eur J Nucl Med Mol* 2008; 35: 1100–1108.
22. Jeong JM, Hong MK, Chang YS, et al. Preparation of a promising angiogenesis PET imaging agent: 68Ga-labeled c(RGDyK)-isothiocyanatobenzyl-1,4,7-triazacyclononane-1,4,7-triacetic acid and feasibility studies in mice. *J Nucl Med* 2008; 49: 830–836.
23. Lang L, Li W, Guo N, et al. Comparison study of [18F]FAl-NOTA-PRGD2, [18F]FPPRGD2, and [68Ga]Ga-NOTA-PRGD2 for PET imaging of U87MG tumors in mice. *Bioconjug Chem* 2011; 22: 2415–2422.
24. Dijkgraaf I, Yim C-B, Franssen GM, et al. PET imaging of αvβ3 integrin expression in tumors with 68Ga-labelled mono-, di- and tetrameric RGD peptides. *Eur J Nucl Med Mol* 2011; 38: 128–137.
25. Hodivala-Dilke K. alphavbeta3 integrin and angiogenesis: A moody integrin in a changing environment. *Curr Opin Cell Biol* 2008; 20: 514–519.
26. Niu G and Chen X. Why integrin as a primary target for imaging and therapy. *Theranostics* 2011; 1: 30–47.
27. Carmeliet P and Jain RK. Molecular mechanisms and clinical applications of angiogenesis. *Nature* 2011; 473: 298–307.
28. Sun Y, Zeng Y, Zhu Y, et al. Application of (68)Ga-PRGD2 PET/CT for alphavbeta3-integrin imaging of myocardial infarction and stroke. *Theranostics* 2014; 4: 778–786.
29. Choi HY, Paeng JC, Kim SK, et al. Imaging of integrin avb3 expression using 68Ga-RGD positron emission tomography in pediatric cerebral infarct. *Mol Imag* 2013; 12: 213–217.
30. Paeng JC, Lee YS, Lee JS, et al. Feasibility and kinetic characteristics of (68)Ga-NOTA-RGD PET for in vivo atherosclerosis imaging. *Ann Nucl Med* 2013; 27: 847–854.
31. Kim JH, Kim YH, Kim YJ, et al. Quantitative positron emission tomography imaging of angiogenesis in rats with forelimb ishemia using 68Ga-NOTA-c(RGDyK). *Angiogenesis* 2013; 16: 837–846.
32. Kim JH, Lee JS, Kang KW, et al. Whole-body distribution and radiation dosimetry of (68)Ga-NOTA-RGD, a positron emission tomography agent for angiogenesis imaging. *Cancer Biother Radiopharm* 2012; 27: 65–71.
33. Minamimoto R, Jamali M, Barkhodari A, et al. Biodistribution of the (1)(8)F-FPPRGD(2) PET radiopharmaceutical in cancer patients: An atlas of SUV measurements. *Eur J Nucl Med Mol* 2015; 42: 1850–1858.
34. Guo N, Lang L, Li W, et al. Quantitative analysis and comparison study of [18F]AlF-NOTA-PRGD2, [18F]FPPRGD2 and [68Ga]Ga-NOTA-PRGD2 using a reference tissue model. *PloS One* 2012; 7: e37506.
35. Zheng K, Liang N, Zhang J, et al. 68Ga-NOTA-PRGD2 PET/CT for integrin imaging in patients with lung cancer. *J Nucl Med* 2015; 56: 1823–1827.
36. Ergul A, Alhusban A and Fagan SC. Angiogenesis: A harmonized target for recovery after stroke. *Stroke* 2012; 43: 2270–2274.
37. Yamauchi H, Higashi T, Kagawa S, et al. Chronic hemodynamic compromise and cerebral ischemic events in asymptomatic or remote symptomatic large-artery intracranial occlusive disease. *Am J Neuroradiol* 2013; 34: 1704–1710.
38. Silvestre JS, Smadja DM and Levy BI. Postischemic revascularization: From cellular and molecular mechanisms to clinical applications. *Physiol Rev* 2013; 93: 1743–1802.
39. Harik SI, Hritz MA and LaManna JC. Hypoxia-induced brain angiogenesis in the adult rat. *J Physiol* 1995; 485: 525–530.
40. Manoonkitiwongsa PS, Jackson-Friedman C, McMillan PJ, et al. Angiogenesis after stroke is correlated with increased numbers of macrophages: The clean-up hypothesis. *J Cereb Blood Flow Metab* 2015; 21: 1223–1231.
41. Ma Y, Zechariah A, Qu Y, et al. Effects of vascular endothelial growth factor in ischemic stroke. *J Neurosci Res* 2015; 90: 1873–1882.
42. Eo JS, Paeng JC, Lee S, et al. Angiogenesis imaging in myocardial infarction using 68Ga-NOTA-RGD PET: Characterization and application to therapeutic efficacy monitoring in rats. *Coronary Artery Dis* 2013; 24: 303–311.